J. Membrane Biol. 67, 63–71 (1982)

The Journal of
Membrane Biology

Small Signal Impedance of Heart Cell Membranes

David E. Clapham* and Louis J. DeFelice
Department of Anatomy, Emory University School of Medicine, Atlanta, Georgia 30322

Summary. The electrical impedance of seven-day ventricular embryonic chick heart cell membranes maintained in tissue culture was measured under voltage clamp using the two-microelectrode voltage-clamp technique. Small sinusoidal perturbations were added to the voltage-clamp potential and the amplitude and phase of the steady-state sinusoidal response in current was recorded as a function of mean clamp potential or perturbing frequency. The experimental results are compared with two models of excitability for heart: the MNT model (McAllister, Noble & Tsien, *J. Physiol. (London)* **251**:1–59, (1975) and the BR model (Beeler & Reuter, *J. Physiol. (London)* **268**:177–210, 1977). The small signal impedance of heart cell membranes, in theory and experiment, shows a resonance near 1 Hz and near the threshold potential. The effect of this resonance is to increase the effective length constant of the membrane for these conditions.

Key words embryonic heart cells · impedance · voltage clamp · beat rate · propagation

Introduction

Cardiac membrane electrophysiology has focused largely on the suprathreshold, nonlinear responses in voltage such as the action potential, or large nonlinear responses in current measured under voltage clamp. Another property of excitable cells is their subthreshold response to small voltage or current perturbations. If the perturbations are small enough, the responses are approximately linear. These small-signal responses have been studied extensively in nerve membrane, and the membrane impedance (or its inverse, the membrane admittance) is well defined. We have looked at the small signal behavior of heart cell membrane under voltage clamp. We report here some consequences of the membrane's ability to filter signals important to the overall function of the heart. Detwiler, Hodgkin and McNaughton (1978) have reported an interesting parallel in vertebrate photoreceptor.

The subthreshold behavior of excitable cell membranes includes a rich array of oscillatory activity. This oscillatory activity can be described by the resistive, inductive, and capacitive (RLC) characteristics of excitable membranes for the linear response in the depolarized range of voltages (Mauro, Conti, Dodge & Schor, 1970). Cole and Baker (1941) first reported an inductive reactance in the squid giant axon membrane. Hodgkin and Huxley (1952) identified the time and voltage-dependent conductance of the ionic channels in the membrane as the source of the inductive reactance. By linearizing the nonlinear differential equations that describe excitability in nerve, Chandler, Fitzhugh and Cole (1962) and Mauro et al. (1970) defined the linear membrane impedance that arises from the voltage-dependent, time-variant conductances of sodium and potassium channels. The equivalent circuit of the membrane has a natural frequency of oscillation, or resonance. Resonant frequencies in nerve membrane have been studied theoretically from a linearization of Hodgkin-Huxley (1952) equations for squid axon, and from the Dodge (1963) and Hille (1967) equations for node of *Ranvier* (Clapham & DeFelice, 1976; Clapham, 1979; DeFelice, 1981).

Although the nonlinear differential equations used to model heart cell membranes are still in transition, present models predict much of the activity of heart electrophysiology. Since subthreshold electronic interaction must depend on the passive membrane impedance, the effect of the voltage and frequency dependent impedance of cardiac membranes on voltage homogeneity may be important in the proper function of the heart. Also, oscillatory activity at resonant frequencies and voltages may play a role in the generation of arrythmias.

In this paper, we compare the measured small

* *Present address:* Department of Medicine, Cardiovascular Division, Brigham and Woman's Hospital, Boston, Massachusetts 02115.

0022-2631/82/0067-0063 $01.80

signal impedance of 7-day chick embryonic ventricular heart cell membrane to the impedance derived by linearizing two well-known models — the 1975 McAllister, Noble and Tsien (MNT) equations for Purkinje fiber and the 1977 Beeler and Reuter equations for mammalian ventricle. The impedance derived from these models agrees reasonably well with the measured membrane impedance and provides a basis for understanding subthreshold behavior of excitable heart cell membranes.

Materials and Methods

Computations

The nonlinear differential equations summarizing voltage-clamp data in Purkinje fibers (McAllister et al., 1975) and in ventricular myocardium (Beeler & Reuter, 1977) were linearized to yield the small signal impedance of the heart cell membrane. The same procedure is outlined in detail for squid axon by Hodgkin and Huxley (1952) and Mauro (1970). Assuming a small perturbation δV we may calculate the response (δI); the small signal impedance is defined as $\delta V/\delta I$. In the MNT model, total membrane current is the sum of nine independent ionic currents plus the capacitative current:

$$I = C\frac{dV}{dt} + i_{\mathrm{Na}} + i_{\mathrm{Na},b} + i_{si} + i_{\mathrm{K}_1} + i_{\mathrm{K}_2} + i_{x_1} + i_{x_2} + i_{qr} + i_{\mathrm{Cl},b}.$$

For a graphical summary of the MNT model *see* Fig. 8 of DeHaan and DeFelice (1978). Briefly, there are four predominant ionic carriers: sodium, potassium, calcium, and chloride. The abbreviations are as follows: Na = sodium; si = slow inward (largely carried by Ca); K = potassium, K_1, K_2, x_1, x_2 are carried largely by potassium; qr = chloride; b = background. Only Na, si, K_2, qr, x_1 and x_2 are controlled by time-dependent conductances. Individual linear circuit elements may be identified with each current. These are summarized in the Appendix.

Electrophysiology

The tissue preparations used in these experiments were aggregates of 7-day chick embryonic ventricular cells described in detail elsewhere (Clapham, Shrier & DeHaan, 1980). Briefly, cells are dissociated in a multiple-cycle trypsinization process. Inocula of 5×10^5 cells are reaggregated in 3 ml of medium 818 A (Sachs & DeHaan, 1973) by gentle gyration for 48 hr. Spheroidal aggregates are formed during gyration; these aggregates range in size from 100 to 300 μm in diameter, and contain 1000 to 3000 cells. Temperature is maintained at 37 °C, with pH of 7.2 under an atmosphere of 5% CO_2, 10% O_2, 85% N_2. Aggregates were transferred from the flask to a Falcon plastic tissue culture dish (Becton, Dickinson and Co., Rutherford, N.J.) for electrophysiological recordings.

Two-microelectrode voltage clamps (Deck, Kerr & Trautwein, 1964; Hecht, Hutter & Lywood, 1964) were performed with circuitry similar to that used by Nathan and DeHaan (1979). Current was measured as the voltage drop across a 10 MΩ feedback resistor of an operational amplifier (Analog Devices, Model 148 K). The bath was clamped through an agar bridge and Ag-AgCl wire. Command sine wave voltages were applied to the summing junction of the clamp amplifier. Current and voltage outputs were recorded on a four-channel FM tape recorder (Hewlett Packard Model 3464) at 3-3/4 ips. In order to measure the voltage and current sinusoids at high gain, a d-c offset was added to the measured signal before recording on magnetic tape. In most experiments, the mean clamp potentials was varied while the frequency of the perturbing sine wave was held constant. In a few experiments, the mean clamp potential was held constant and the frequency of the perturbing sine wave was varied. In all experiments, external K was 4.8 mM. Tetrodotoxin (TTX) (Sigma Chemical Co., St. Louis, Mo.) was added to the bath at a concentration of 10^{-6} g/ml to block the fast inward Na current. The peak-to-peak amplitude and the frequency of the perturbing voltage were kept below 2 mV and 10 Hz.

Results

Theoretical

The impedance of the MNT Purkinje fiber was calculated for frequencies between 0 and 5 Hz and for voltages between 0 and −100 mV (absolute membrane potentials, negative inside with respect to outside). To summarize, $|Z|$ (Fig. 1*a*) and phase (Fig. 1*b*) are plotted as functions of both voltage and frequency in three-dimensional perspective. Figures 1*a* and 1*b* are for the full MNT membrane, including the fast Na current. Voltage varies in 1 mV intervals. Frequency varies in 0.05 Hz intervals. There are three large resonances in the impedance plot. Peaks occur at frequencies below 2 Hz. The first resonance (from the hyperpolarized side) occurs at −76 mV, near threshold for Purkinje fiber. The resonant peaks have extremely steep voltage and frequency dependence. Around −76 mV the slopes are ~27 kΩ cm²/mV for voltage and ~300 kΩ cm²/Hz for frequency.

Figure 2*b* shows the phase of the complex impedance for the linearized MNT model over the same range used for Z in Fig. 1*a*. The left origin corresponds to 0 phase shift. Positive phase means current lags voltage. For very negative potentials the phase shift is zero. Phase is negative between −100 and −76 mV and between −36 and 0 mV. Phase is positive between −87 and −38 mV above 1 Hz.

The equivalent small signal impedance of the cardiac membrane is the result of parallel elements that may be grouped into the Na system, the K system, etc. The impedance of the MNT membrane, excluding i_{Na}, i_{si}, and i_{qr}, shows two broad resonances at −63 mV (centered around 0.45 Hz), and −37 mV (0.05 to 0.7 Hz). The linearized Noble (1962) equations have only one broad resonance at −50 mV (2.5 Hz) if $I_{\mathrm{Na}} = 0$ (DeHaan & DeFelice, 1978; Clapham, 1979). The impedance of the MNT model with $I_{\mathrm{Na}} = 0$ (Fig. 1*c*) has three resonances. It is similar to Fig. 1*a* but with an increase in amplitude of the impedance and a shift of the most de-

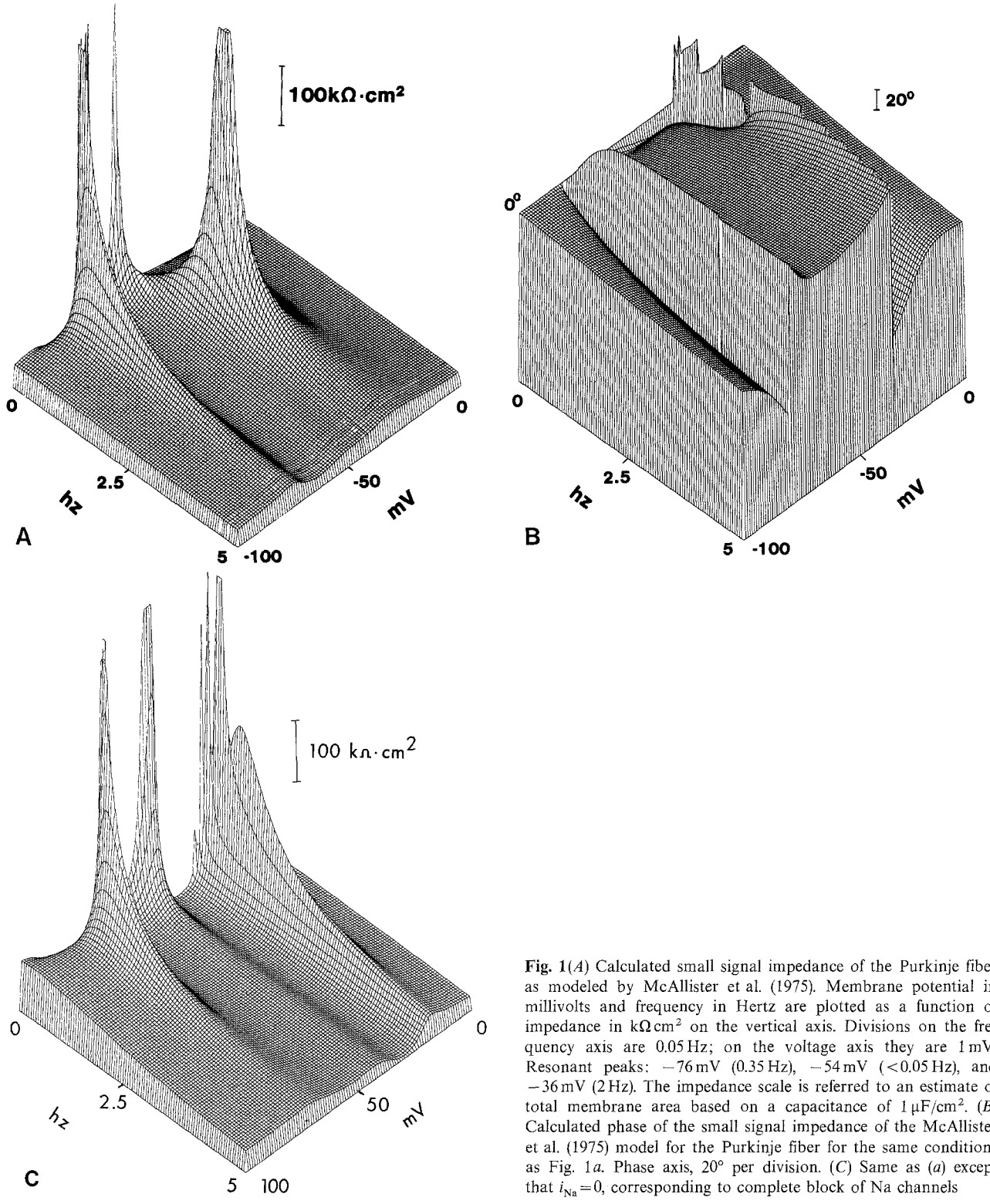

Fig. 1(*A*) Calculated small signal impedance of the Purkinje fiber as modeled by McAllister et al. (1975). Membrane potential in millivolts and frequency in Hertz are plotted as a function of impedance in $k\Omega cm^2$ on the vertical axis. Divisions on the frequency axis are 0.05 Hz; on the voltage axis they are 1 mV. Resonant peaks: −76 mV (0.35 Hz), −54 mV (<0.05 Hz), and −36 mV (2 Hz). The impedance scale is referred to an estimate of total membrane area based on a capacitance of 1 $\mu F/cm^2$. (*B*) Calculated phase of the small signal impedance of the McAllister et al. (1975) model for the Purkinje fiber for the same conditions as Fig. 1*a*. Phase axis, 20° per division. (*C*) Same as (*a*) except that $i_{Na}=0$, corresponding to complete block of Na channels

polarized resonance to lower frequency. The peaks in the MNT ($I_{Na}=0$) model are −70 mV (0.5 Hz), −42 mV, (<0.001 Hz) and −17 mV (0.1 Hz).

The Beeler-Reuter model describes excitability in adult ventricular heart cells. This model has a Na current, a Ca current and two K currents. Figures 2*a* and 2*b* shows the results of linearization of the BR equations. Three resonant peaks occur: −81 mV (0.2 Hz), −34 mV (0.0001 Hz), and −29 mV (1.4 Hz). At −81 mV the slopes around the membrane are

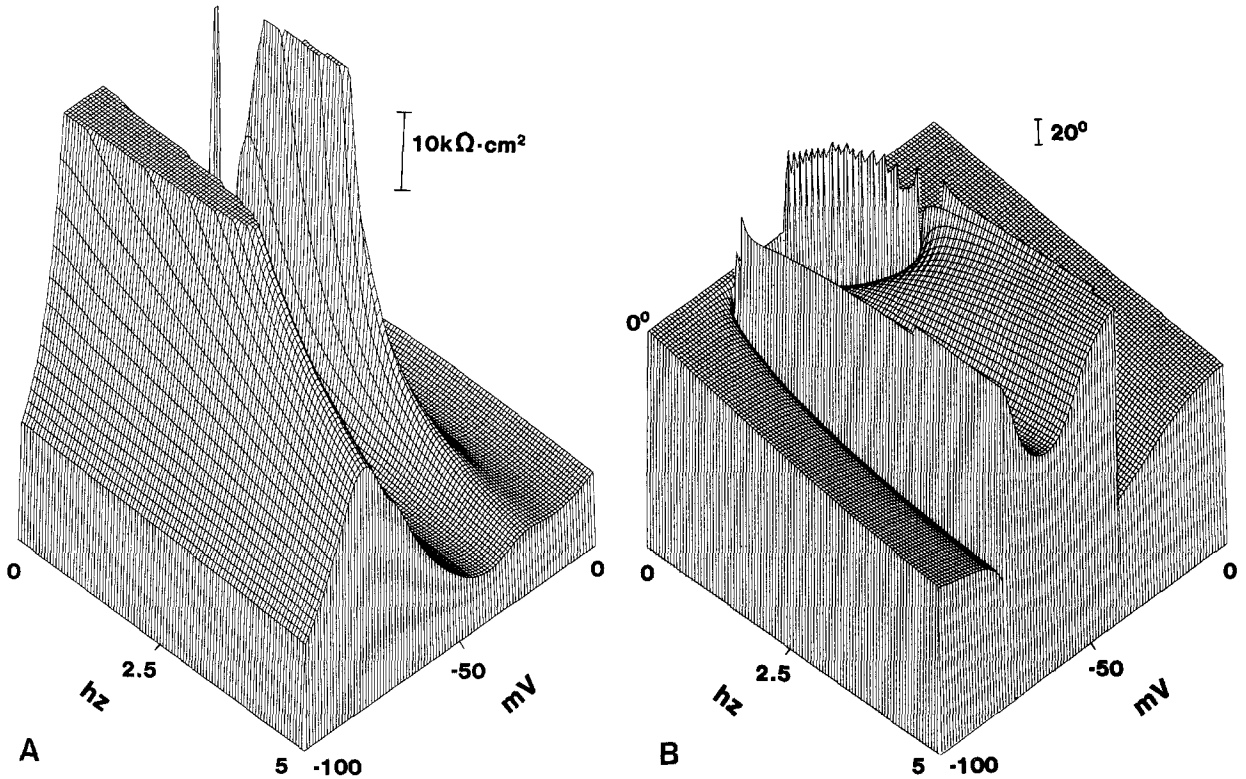

Fig. 2(*A*) Calculated small signal impedance of heart ventricular cells as modeled by Beeler and Reuter (1977). Three resonant peaks occur: −81 mV (0.2 Hz), −34 mV (0.0001 Hz), and −29 mV (1.4 Hz). Impedance scale 10 kΩ cm². Small divisions on the frequency axis are 0.05 Hz; on the voltage axis they are 1 mV. Impedance scale referred to total membrane area. (*B*) Calculated phase of the small signal impedance of the Beeler-Reuter model for ventricle tissue. Phase axis, 20° per division

$\sim 8\,k\Omega\,cm^2/mV$ for voltage and $\sim 20\,k\Omega\,cm^2/Hz$ for frequency.

Experiments

Ventricular aggregates of 7-day embryonic chick ventricle were voltage clamped at various potentials and a 1 mV sine wave of various frequencies was applied to measure the impedance of the membrane. Holding potentials were changed in approximately 2 mV steps at constant frequency. Alternatively, holding potential was held constant while the frequency was varied. A total of 21 experiments were conducted on five different aggregates.

Figure 3 shows the results of one experiment. At −84 mV (resting membrane potential) voltage and current traces were in phase for a frequency of 2 Hz. With depolarization to −77 mV, the current at 2 Hz is dramatically decreased (impedance increases) and the phase shift between voltage and current is −90°. Further depolarization to −64 mV results in an increase in current (decrease in impedance) and a phase shift to −180°.

Figure 4*a* shows the measured $I-V$ curve for the aggregate as compared to the MNT and BR models. The $I-V$ curves are steady-state curves measured 4 sec after the voltage step was applied. In 4*b* the measured aggregate impedance at $f=2$ Hz is plotted as a function of voltage and is compared to the linearized models. The fast Na current is blocked in the models ($i_{Na}=0$) to correspond to experimental conditions. With blocked Na channels (11^{-5} μg/ml TTX) both models and the experiment show a fivefold increase in impedance. Predictably, the BR model peak is hyperpolarized with respect to the MNT model since K_o^+ is 2.5 in the Purkinje model and 5.4 mM in the mammalian ventricle model. In 4*c* the phase of both models is compared to the measured phase. Both models predict a sudden jump in phase from −90 to +90 as the membrane is depolarized; the aggregate membrane jumps from 0° to −180°. Phase shifts at the resonance are extremely sensitive to the conditions of the test, both in the model and in the experiments. Phase changes in the experiment did not reproduce either model well, especially near resonance.

Figure 5 summarizes results from another aggregate when voltage and frequency are varied.

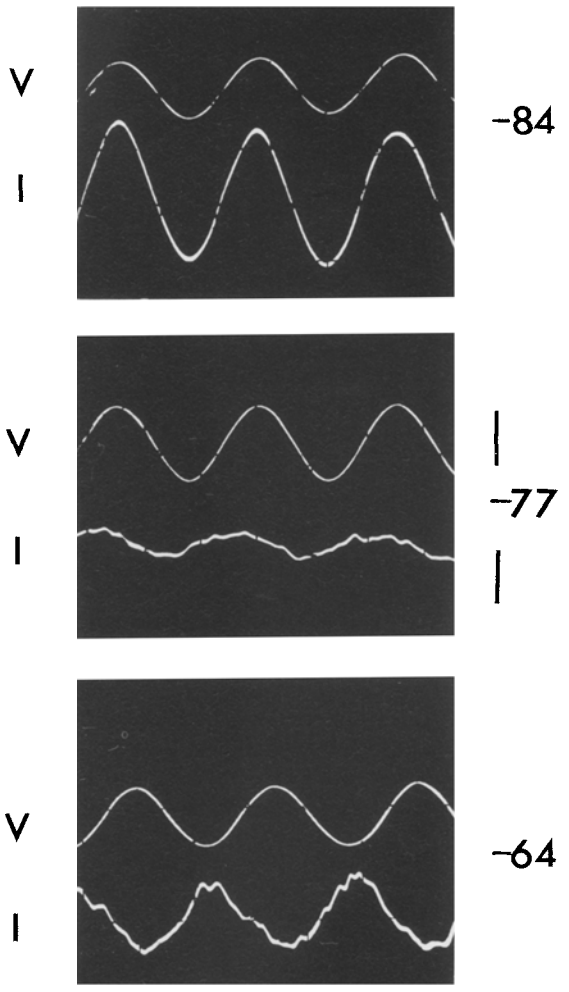

Fig. 3. Voltage and current trace from a 7-day heart cell aggregate voltage clamped to three different potentials. Total membrane surface area: 2×10^{-3} cm^2. Rest potential: -84 mV. Scales: 1.1 mV and 1.0 nA. The threshold for beating was -77 mV at $f = 2$ Hz. Note the increase in impedance around threshold

There is a rise in the impedance along the frequency axis with a peak at around 2 Hz. The impedance is largely capacitive by 10 Hz and falls rapidly with frequency. On the voltage axis, the capacitance dominates in the hyperpolarizing direction. As the membrane is depolarized, impedance rises sharply to a peak around -76 mV, approximately threshold in this preparation. Generally, the impedance is highest near the threshold voltage and near the beat frequency of the heart. This is in qualitative agreement with the models.

Resonance and Length Constants

Eisenberg, Barcilon and Mathias (1979; EBM model) have derived the relationship between the voltage distribution in a spherical syncytium and the tissue parameters that describe the syncytium. The model is applicable to spherical preparations like the heart cell aggregate. As they point out, the cleft spaces between cells form resistive pathways to the inner membranes, and therefore the syncytium is never isopotential. Current flowing across the inner membranes into deep cleft spaces must drop across the distributed impedance of the clefts. The result is that the transmembrane voltage for a central cell is different than for a cell on the edge of the syncytium. Calculations using the EBM model with morphological parameters of aggregates show that the expected voltage differences (deviations from isopotential) are extremely small at low frequencies (<10 Hz) (Clapham, 1979; Clay, DeFelice & DeHaan, 1979). We wish to emphasize that the resonance of the heart cell membrane makes the deviations from voltage homogeneity even smaller. Voltage drops across the cell membrane are relatively larger, around 1–2 Hz, compared to voltage drops in the cleft. In effect, the resonance acts to increase voltage homogeneity near 1 Hz.

Eisenberg et al. (1979) define a propagation constant $\gamma^2(j\omega)$ which is analogous to the inverse of the length constant at zero frequency.

$$\gamma^2(j\omega) = (R_i + R_e)\left(\frac{S_m}{V_t}\right)_{Y_m}$$

where $\omega = 2\pi f$, R_i = resistivity of the intracellular medium (Ω cm), R_e = resistivity of the extracellular medium (Ω cm), S_m/V_t = surface-to-volume ratio of the aggregate (cm^{-1}), Y_m = admittance of the membrane $= \frac{1}{Z_m(\mathrm{K}\Omega\,\mathrm{cm}^2)}$. S_m/V_t for the aggregate is 4440 cm^{-1} (Clapham, 1979). R_i and R_e are best defined by curve fitting electrophysiologic data as discussed by Mathias et al. (1979). If we estimate $R_i = 600\,\Omega$ cm, $R_e = 1000\,\Omega$ cm, then $1/\gamma^2$ is known directly from Fig. 5 by scaling the impedance axis. The inverse of the propagation constant (using our assumptions) is $\frac{\sqrt{Z}}{1.0084}$ microns where Z is in units of kilohms. For membrane impedance of 30 kΩ cm^2 (near the peak) the frequency-dependent length constant is 652 μ. For an impedance of 1 kΩ cm^2 (on either side of the peak) it is 119 μ. Voltages at frequencies near 1 Hz are seen by the membrane 6 times farther away than voltages at higher or lower frequencies. In effect, the membrane reinforces signals at frequencies near the beating frequency of heart tissue and suppresses higher and lower frequencies. Similarly, the length constant is longest at voltages just below the stimulating voltage. In summary, the tissue has its greatest voltage homogeneity at 1–2 Hz near threshold.

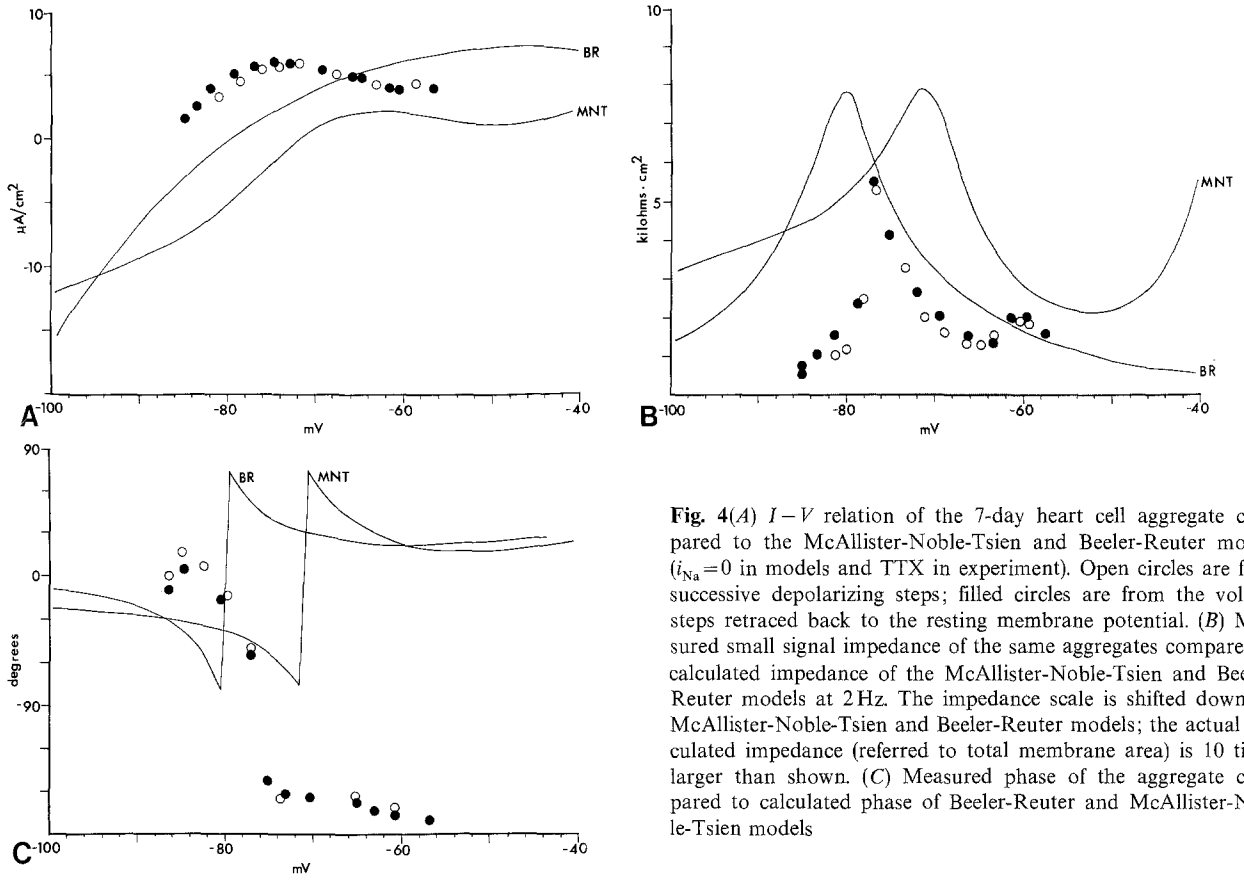

Fig. 4(*A*) $I-V$ relation of the 7-day heart cell aggregate compared to the McAllister-Noble-Tsien and Beeler-Reuter models ($i_{Na}=0$ in models and TTX in experiment). Open circles are from successive depolarizing steps; filled circles are from the voltage steps retraced back to the resting membrane potential. (*B*) Measured small signal impedance of the same aggregates compared to calculated impedance of the McAllister-Noble-Tsien and Beeler-Reuter models at 2 Hz. The impedance scale is shifted down for McAllister-Noble-Tsien and Beeler-Reuter models; the actual calculated impedance (referred to total membrane area) is 10 times larger than shown. (*C*) Measured phase of the aggregate compared to calculated phase of Beeler-Reuter and McAllister-Noble-Tsien models

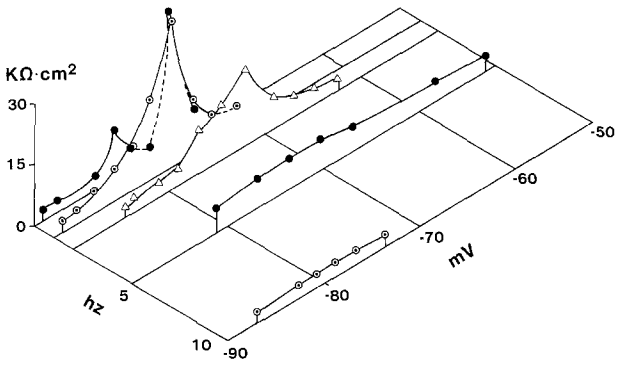

Fig. 5. Measured impedance of a heart cell aggregate in TTX as a function of frequency and voltage (*see* Fig. 1*c* for comparison to theory). The impedance is derived from sine wave voltage clamp at various potentials at the frequencies shown. Total membrane area: $7.7\times10^{-3}\,\mathrm{cm}^2$

Discussion

The embryonic heart cell aggregate beats spontaneously at a rate between 1 and 2 Hz. In this frequency range the membrane impedance exhibits a resonance; this resonance exists in both voltage and frequency and defines a highly localized maximum impedance around −75 mV between 1 and 2 Hz. In TTX, the aggregates beat with a frequency between 2 and 3 Hz when depolarized from rest by a few millivolts.

Our experiments show that the cardiac membrane is most likely to beat at its resonant frequency. This is similar to the squid axon, which can be induced to fire a train of action potentials at its resonant frequency ($\simeq$100 Hz, −54 mV; Mauro et al., 1970) and to the node of *Ranvier* (Bromm, 1975; Clapham & DeFelice, 1976; DeHaan & DeFelice, 1978). In each case, the linear models predict the most excitable points in the frequency-voltage plane.

A resonance near 1 Hz has a significant effect on subthreshold electronic interaction in heart tissue. Frequency components of signals around 1 Hz affect a larger area of the membrane than components at higher or lower frequency. In other words, voltage homogeneity is frequency dependent, and frequencies other than the resonant frequency are damped. The net effect of the resonant property of cardiac membranes is the entrainment of heart cells at this frequency. Detwiler et al. (1978) have reported a similar effect of membrane impedance on the electronic response of vertebrate photoreceptors. The effect of an RLC response of the photoreceptor is to increase the length constant for high frequency sti-

muli. The effect of the RLC response of the heart membrane is to enhance homogeneity at the beat frequency and near threshold.

Although the data and model correspond qualitatively, a discrepancy exists in specific impedance values. The linearized MNT model was calculated using the original assignment of cylindrical surface of the Purkinje fiber. Actually, the enfolded surface area is about 10 times larger (McAllister et al., 1975). Thus, all calculated impedance values should be multiplied by 10. The values of specific impedance for the aggregates are lower than expected. Also, the values of specific dc resistance are lower than in the study carried out on aggregates in 1977 by Clay et al. (1979). In the Clay et al. study, R_m was 18.5 kΩ cm^2 for voltages between −66 and −70 mV. There are several reasons for the discrepancy between these results. First, $[K_o^+]$ was 4.8 mM in the present study and 4.5 mM in the earlier study. Second, a new crystalline trypsin was used in the disaggregation medium in the present studies, which possibly altered the membrane characteristics from previous work. The resting membrane potential is near −85 mV in our experiments versus −65 to −70 mV in the earlier experiments. In Clay et al. (1979) a sharp increase in dc resistance occurs at −60 mV. This corresponds to the sharp increase near −75 mV in our experiments. These characteristics of our membrane appear shifted by 15 mV with respect to the earlier study. Our values of membrane resistance are consistent with extrapolated values of resistance to a more hyperpolarized voltage in the Clay et al. (1979) study.

One of the main differences between BR and MNT models is the absence of i_{K_2} in the BR model. In the hyperpolarized range the difference in impedance between models is slight. In this range impedance elements contributed by i_{K_1} are much smaller in magnitude than i_{K_2} elements. Since they are in parallel, lower impedance elements dominate the total impedance.

Ideally a complete model for heart cell aggregates could be linearized to compare with our experimental data. However, voltage-clamp data are as yet incomplete for our preparation. Sodium, slow inward (Nathan & DeHaan, 1979) and pacemaker currents (Clay & Shrier, 1981) have been described, but other currents probably exist that have not yet been characterized. For this reason we have linearized two well-known models for comparison with our data. Although the MNT and BR models do not predict the impedance surface of embryonic heart cells with precision, good qualitative agreement on the location of the resonant points exists. Disagreement between specifics of the heart cell aggregate and the linearized MNT and BR models are not surprising since they describe different tissues. The purpose of this paper is to show that the resonance in membrane near 1 Hz and the resonance in impedance near threshold are seen in heart tissue, and that cardiac tissue examined in theory or experiment are qualitatively similar in this regard.

Appendix

We have calculated the circuit elements of the equivalent circuit of the MNT Purkinje cell membrane. (*See* McAllister et al. (1975) for original notation.) Consider a variation in I, V and g at a given steady state and linearize by retaining only first-order terms (*see* Mauro et al., 1970). The impedance ($\delta V/\delta I$) of the small signal response may be separated into R, L and C elements. All values of m, h, etc., and all derivatives of α_m, β_m, etc., are at constant V. The equivalent circuit is a parallel network of elements with each r and L of each subscript being in series. R and C elements are each in parallel to rL branches. Units of R and r are Ω cm^2. Units of inductance are Ω sec cm^2 = henry cm^2.

The sodium current of the MNT model described by $i_{Na} = \bar{g}_{Na}(E - E_{Na}) m^3 h$ yields one simple resistor (R_{Na}) and four voltage-dependent elements (r_m, L_m, r_h, L_h). $R_{Na,b}$ is a consequence of the background sodium current.

$$R_{Na,b} = \frac{1}{\bar{g}_{Na,b}} \qquad R_{Na} = \frac{1}{\bar{g}_{Na} m^3 h}$$

$$r_m = \frac{\alpha_m + \beta_m}{3\bar{g}_{Na} m^2 h (V - V_{Na}) \left[\left(\frac{d\alpha_m}{dV}\right) - m\left(\frac{d(\alpha_m - \beta_m)}{dV}\right)\right]}$$

$$L_m = \frac{r_m}{\alpha_m + \beta_m}$$

$$r_h = \frac{\alpha_h + \beta_h}{\bar{g}_{Na} m^3 (V - V_{Na}) \left[\left(\frac{d\alpha_h}{dV}\right) - h_v\left(\frac{d\alpha_h - d\beta_h}{dV}\right)\right]}$$

$$L_h = \frac{r_h}{\alpha_h + \beta_h}.$$

There are three separate time- and voltage-dependent potassium currents in the MNT model. For the pacemaker current $i_{K_2} = \bar{i}_{K_2} \cdot s$ where

$$\bar{i}_{K_2} = \frac{2.8 \exp[0.04(E + 110)] - 1}{\exp[0.08(E + 60)] + \exp[0.04(E + 60)]}$$

$$R_{K_2} = \frac{1}{s \frac{d}{dV}(\bar{i}_{K_2})}$$

$$r_s = \frac{\alpha_s + \beta_s}{\bar{i}_{K_2}\left[\left(\frac{d\alpha_s}{dV}\right) - s\left(\frac{d(\alpha_s + \beta_s)}{dV}\right)\right]}$$

$$L_s = \frac{r_s}{\alpha_s + \beta_s}.$$

The plateau potassium current i_{x_1} has the form $i_{x_1} = \bar{i}_{x_1} \cdot x_1$ where

$$\bar{i}_{x_1} = \frac{1.2 \exp[0.04(E + 95)] - 1}{\exp[0.04(E + 45)]}$$

$$R_{x_1}=\frac{1}{\overline{i_{x_1}}\left[\frac{d(\overline{i_{x_1}})}{dV}\right]}$$

$$r_{x_1}=\frac{\alpha_{x_1}+\beta_{x_1}}{\overline{i_{x_1}}\left[\left(\frac{d\alpha_{x_1}}{dV}\right)-x_1\left(\frac{d(\alpha_{x_1}+\beta_{x_1})}{dV}\right)\right]}$$

$$L_{x_1}=\frac{r_{x_1}}{\alpha_{x_1}+\beta_{x_1}}.$$

The second plateau potassium current, $i_{x_2}=\overline{i_{x_2}}\cdot x_2$ where $\overline{i_{x_2}}=25+0.385\,V$

$$R_{x_2}=\frac{1}{\overline{i_{x_2}}\left[\frac{d(\overline{i_{x_2}})}{dV}\right]}.$$

The slow inward (calcium) current, $i_{si}=\bar{g}_{si}(E-E_{si})\,d\cdot f$ yields one simple resistance and four voltage-dependent elements:

$$R_{si}=\frac{1}{\bar{g}_{si}\,df}$$

$$r_d=\frac{\alpha_d+\beta_d}{\bar{g}_{si}\,f(V-V_{si})\left[\left(\frac{d\alpha_d}{dV}\right)-d\left(\frac{d(\alpha_d+\beta_d)}{dV}\right)\right]}$$

$$L_d=\frac{r_d}{\alpha_d+\beta_d}$$

$$r_f=\frac{\alpha_f+\beta_f}{\bar{g}_{si}\,d(V-V_{si})\left[\left(\frac{d\alpha_f}{dV}\right)-f\left(\frac{d(\alpha_f+\beta_f)}{dV}\right)\right]}$$

$$L_f=\frac{r_f}{\alpha_f+\beta_f}.$$

Note: The d' term of the "residual i_{si}" has been omitted since the resistance derived from d' does not change the total impedance.

The transient chloride current is also time- and voltage-dependent, where $i_{qr}=\bar{g}_{qr}(E-E_{Cl})\cdot q\cdot r$. The background chloride current contributes a simple resistor $R_{Cl,b}$.

$$R_{qr}=\frac{1}{\bar{g}_{qr}\,qr}$$

$$r_q=\frac{\alpha_q+\beta_q}{\bar{g}_{qr}\,r(V-V_{Cl})\left[\left(\frac{d\alpha_q}{dV}\right)-q\left(\frac{d(\alpha_q+\beta_q)}{dV}\right)\right]}$$

$$L_q=\frac{r_q}{\alpha_q+\beta_q}$$

$$r_r=\frac{\alpha_r+\beta_r}{\bar{g}_{qr}\,q(V-V_{Cl})\left[\left(\frac{d\alpha_r}{dV}\right)-r\left(\frac{d(\alpha_r+\beta_r)}{dV}\right)\right]}$$

$$L_r=\frac{r_r}{\alpha_r+\beta_r}$$

$$R_{Cl,b}=\frac{1}{g_{Cl,b}}.$$

The linearization process was also carried out for the Beeler-Reuter model (1977), which incorporates only four currents: $I=\frac{dv}{Cdt}+i_{Na}+i_s+i_{x_1}+i_{K_1}$. The dependence of i_s on Ca^{++} was handled by a modification of i_s and i_{x_1} as suggested by Beeler and Reuter (1977); E_s was fixed at $+40\,mV$; $\bar{g}_s$ was multiplied by 2.2 and i_{x_1} multiplied by 1.9.

Linearization of the background and time-dependent sodium currents: $i_{Na}=(\bar{g}_{Na}\,m^3\,hj+g_{NaC})(V-E_{Na})$ yields the circuit elements listed below. The second inactivation parameter j yields two new elements.

$$R_{NaC}=\frac{1}{\bar{g}_{NaC}}\qquad R_{Na}=\frac{1}{g_{Na}\,m^3\,hj}$$

$$r_m=\frac{\alpha_m+\beta_m}{3\bar{g}_{Na}\,m^2\,hj(V-V_{Na})\left[\left(\frac{d\alpha_m}{dV}\right)-m\left(\frac{d(\alpha_m+\beta_m)}{dV}\right)\right]}$$

$$L_m=\frac{r_m}{\alpha_m+\beta_m}$$

$$r_h=\frac{\alpha_h+\beta_h}{\bar{g}_{Na}\,m^3j(V-V_{Na})\left[\left(\frac{d\alpha_h}{dV}\right)-h\left(\frac{d(\alpha_h+\beta_h)}{dV}\right)\right]}$$

$$L_h=\frac{r_h}{\alpha_h+\beta_h}$$

$$r_j=\frac{\alpha_j+\beta_j}{\bar{g}_{Na}\,m^3h(V-V_{Na})\left[\left(\frac{d\alpha_j}{dV}\right)-j\left(\frac{d(\alpha_j+\beta_j)}{dV}\right)\right]}$$

$$L_j=\frac{r_j}{\alpha_j+\beta_j}.$$

The outward currents in ventricle include one time-independent background current i_{K_1} plus one time-dependent outward current i_{x_1}.

$$i'_{K_1}=(0.35)\frac{4\exp[0.04(V_m+85)-1]}{\exp[0.08(V_m+53)]+\exp[0.04(V_m+53)]}$$

$$i''_{K_1}=\frac{0.2(V_m+23)}{1-\exp[-0.04(V_m+23)]}\qquad \text{where } i_{K_1}=i'_{K_1}+i''_{K_1}$$

so

$$R'_{K_1}=\frac{1}{\frac{d}{dV}(i'_{K_1})}\qquad R''_{K_1}=\frac{1}{\frac{d}{dV}(i''_{K_1})}.$$

Let

$$i_{x_1}=\frac{0.8\exp[0.04(V_m+77)]-1}{\exp[0.04(V_m+35)]}$$

then

$$R_{x_1}=\frac{1}{\frac{d}{dV}(i_{x_1})\cdot x_1}$$

$$r_{x_1}=\frac{\alpha_{x_1}+\beta_{x_1}}{i_{x_1}\left[\left(\frac{d\alpha_{x_1}}{dV}\right)-x_1\left(\frac{d(\alpha_{x_1}+\beta_{x_1})}{dV}\right)\right]}$$

$$L_{x_1}=\frac{r_{x_1}}{\alpha_{x_1}+\beta_{x_1}}.$$

The slow inward current is a time-dependent current carried by calcium ions, where $i_s=\bar{g}_s\,df(V-E_s)$.

$$r_d=\frac{\alpha_d+\beta_d}{\bar{g}_s\cdot f(V-70)\left[\left(\frac{d\alpha_d}{dV}\right)-d\left(\frac{d(\alpha_d+\beta_d)}{dV}\right)\right]}$$

$$L_d=\frac{r_d}{\alpha_d+\beta_d}$$

$$r_f=\frac{\alpha_f+\beta_f}{\bar{g}_s\cdot d(V-70)\left[\left(\frac{d\alpha_f}{dV}\right)-f\left(\frac{d(\alpha_f+\beta_f)}{dV}\right)\right]}$$

$$L_f=\frac{r_f}{\alpha_f+\beta_f}$$

$$R_{Ca}=\frac{1}{\bar{g}_s\,df}.$$

References

Beeler, G.W., Reuter, H. 1977. Reconstruction of the action potential of ventricular myocardial fibres. *J. Physiol. (London)* **268**:177–210

Bromm, B. 1975. Spike frequency of the nodal membrane generated by high frequency alternating current. *Pfluegers Arch.* **353**:1–19

Chandler, W.K., Fitzhugh, R., Cole, K.S. 1962. Theoretical stability properties of a space clamped axon. *Biophys. J.* **2**:105–127

Clapham, D.E. 1979. A Whole Tissue Model of the Heart Cell Aggregate; Electrical Coupling Between Cells, Membrane Impedance and the Extracellular Space. Doctoral Dissertation, Emory University, Atlanta, Georgia

Clapham, D.E., DeFelice, L.J. 1976. The theoretical small signal impedance of the frog node *Rana pipiens*. *Pfluegers Arch.* **366**:273–276

Clapham, D.E., Shrier, A., DeHaan, R.L. 1980. Junctional resistance and action potential delay between embryonic heart cell aggregates. *J. Gen. Physiol.* **75**:633–654

Clay, J.R., DeFelice, L.J., DeHaan, R.L. 1979. Current noise parameters derived from voltage noise and impedance in embryonic heart cell preparations. *Biophys. J.* **28**:169–184

Clay, J.R., Shrier, A. 1981. Analysis of subthreshold pacemaker currents in chick embryonic heart cells. *J. Physiol. (London)* **312**:471–490

Cole, K.S., Baker, R.F. 1941. Transverse impedance of the squid giant axon during current flow. *J. Gen. Physiol.* **24**:535–549

Deck, K.A., Kerr, R., Trautwein, W. 1964. Voltage clamp technique in mammalian cardiac fibres. *Pfluegers Arch. Gesamte Physiol.* **280**:50–62

DeFelice, L.J. 1981. Introduction to Membrane Noise. Plenum Press, New York (*See* Chapter 6 and Figs. 87.1 through 87.4, in particular.)

DeHaan, R.L., DeFelice, L.J. 1978. Oscillatory properties and excitability of the heart cell membrane. *Theor. Chem.* **4**:181–233

Detwiler, P.B., Hodgkin, A.L., McNaughton, P.A. 1978. A surprising property of electrical spread in the network of rods in the turtle's retina. *Nature (London)* **274**:562–565

Dodge, F.A. 1963. A Study of Ionic Permeability Changes Underlying Excitation in Myelinated Nerve Fibres of the Frog. Ph.D. Thesis, The Rockefeller University, New York N.Y. (Univ. Microfilms, Ann Arbor, Michigan, No. 63–7333)

Eisenberg, R.S., Barcilon, V., Mathias, R.T. 1979. Electrical properties of spherical syncytia. *Biophys. J.* **30**:151–180

Hecht, H.H., Hutter, O.F., Lywood, D.W. 1964. Voltage-current relation of short Purkinje fibres in sodium deficient solution. *J. Physiol. (London)* **170**:5P–7P

Hille, B. 1967. A Pharmacological Analysis of the Ionic Channels of Nerve. Ph.D. Thesis, The Rockefeller University, New York, N.Y. (Univ. Microfilms, Ann Arbor, Michigan, No. 68–9584)

Hodgkin, A.L., Huxley, A.F. 1952. A quantitative description of membrane current and its application to conduction and excitation in nerve. *J. Physiol. (London)* **117**:500–544

Mauro, A., Conti, F., Dodge, F., Schor, R. 1970. Subthreshold behavior and phenomenological impedance of the squid giant axon. *J. Gen. Physiol.* **55**:497–523

McAllister, R.E., Noble, D., Tsien, R.W. 1975. Reconstruction of the electrical activity of cardiac Purkinje fibers. *J. Physiol. (London)* **251**:1–59

Nathan, R.D., DeHaan, R.L. 1979. Voltage clamp analysis of embryonic heart cell aggregates. *J. Gen. Physiol.* **73**:175–198

Noble, D. 1962. A modification of the Hodgkin-Huxley equations applicable to Purkinje fibre action and pacemaker potentials. *J. Physiol. (London)* **160**:317–352

Sachs, H.G., DeHaan, R.L. 1973. Embryonic myocardial cell aggregates: Volume and pulsation rate. *Dev. Biol.* **30**:233–240

Received 1 July 1981; revised 18 November 1981